telecom

MDPI

Article

Designing Smart Electromagnetic Environments for Next-Generation Wireless Communications

Andrea Massa [1,2,3,*,†], Arianna Benoni [1,†], Pietro Da Rù [1,†], Sotirios K. Goudos [4,†], Baozhu Li [5,†], Giacomo Oliveri [1,†], Alessandro Polo [1,†], Paolo Rocca [1,6,†] and Marco Salucci [1,†]

1 Consorzio Nazionale Interuniversitario per le Telecomunicazioni (CNIT)—"University of Trento" Research Unit, Via Sommarive 9, I-38123 Trento, Italy; arianna.benoni@unitn.it (A.B.); pietro.daru@studenti.unitn.it (P.D.R.); giacomo.oliveri@unitn.it (G.O.); alessandro.polo.1@unitn.it (A.P.); paolo.rocca@unitn.it (P.R.); marco.salucci@unitn.it (M.S.)
2 ELEDIA Research Center (ELEDIA@UESTC), School of Electronic Engineering, University of Electronic Science and Technology of China, Chengdu 611731, China
3 ELEDIA Research Center (ELEDIA@TSINGHUA), Tsinghua University, 30 Shuangqing Road, Haidian, Beijing 100084, China
4 ELEDIA Research Center (ELEDIA@AUTH), Aristotle University of Thessaloniki, 54124 Thessaloniki, Greece; sgoudo@physics.auth.gr
5 Beijing National Research Center for Information Science and Technology (BNRist), Tsinghua University, 30 Shuangqing Road, Haidian, Beijing 100084, China; libaozhu@mail.tsinghua.edu.cn
6 ELEDIA Research Center (ELEDIA@XIDIAN), Xidian University, P.O. Box 191, No. 2 South Tabai Road, Xi'an 710071, China
* Correspondence: andrea.massa@unitn.it; Tel.: +39-0461-282057
† These authors contributed equally to this work.

Abstract: The design of a smart electromagnetic (EM) environment for next-generation wireless communication systems is addressed in this work. The proposed approach aims at synthesizing a desired EM field distribution over a target region, where the receiving terminals are located, through the opportunistic exploitation of the complex scattering interactions between the EM field generated by a reconfigurable primary source and the objects/scatterers present in the environment, which behave as application-driven passive metastructures. The effectiveness and the potentialities of the proposed design methodology are assessed with a proof-of-concept numerical result obtained by means of advanced and reliable simulation tools.

Keywords: smart EM environment; opportunistic sources design; particle swarm optimization

check for updates

Citation: Massa, A.; Benoni, A.; Rù, P.D.; Goudos, S.K.; Li, B.; Oliveri, G.; Polo, A.; Rocca, P.; Salucci, M. Designing Smart Electromagnetic Environments for Next-Generation Wireless Communications. *Telecom* **2021**, *2*, 213–221. https://doi.org/10.3390/telecom2020014

Academic Editor: Gino Sorbello

Received: 30 March 2021
Accepted: 6 May 2021
Published: 12 May 2021

1. Introduction and Motivation

Nowadays, we are witnessing a wide and multidisciplinary debate on the next-generation wireless standard [1,2] after the advent of the fifth-generation (5G) communications systems based on the following statement. The exponential growth of the mobile data traffic that we experimented with in recent decades is expected to further increase in the next years. Indeed, future wireless applications and services (e.g., autonomous vehicles, real-time remote health care, and intelligent industrial automation, just to mention a few [2]), will require higher capacity, lower latency, and higher reliability than those achievable with the 5G standard. Moreover, the need to provide a massive access and ubiquitous wireless coverage will also impose severe energy-efficiency constraints. The wireless infrastructures for future generation mobile communications systems will have to fit such challenging requirements for guaranteeing unprecedented link performance levels, while minimizing the complexity, the power consumption, and the costs of the communication architecture [3–8].

Until nowadays, the base-station (BTS) antennas and the user terminals have been considered as the key players for fostering the technological evolution of the radio access

to the mobile communications network. In this framework, unconventional and cost-effective antenna solutions for both mobile terminals [9] and BTSs [10–12] have been proposed. However, new architectural solutions, alternative to the classical approaches that achieve better coverage and higher data throughput by using more power and more emissions of electromagnetic waves, are required because of the electromagnetic congestion. For instance, by implementing a *Smart Electromagnetic Environment* as an evolution of the standard concepts of wireless infrastructure and wireless channel. Indeed, while traditional communication systems focus the radiated power along the direction of the end-user terminals in order to maximize the link quality and the overall system capacity by increasing the antenna gain and lowering the sidelobe level (SLL) [13], the maximization of the signal-to-noise ratio for next generation wireless networks can be yielded by spatially distributing the radiated power to constructively exploit the wave scattering phenomena in the multipath propagation environment, regardless of the gain, the SLL, or the presence of grating lobes. Towards this end, the design of BTS antennas is carried out by considering the overall end-to-end capacity as the metric to be optimized rather than the standard free-space radiation features (e.g., antenna gain, SLL) [14].

More recently, the idea that the EM environment is a fundamental and key-enabling actor for achieving the challenging objectives foreseen in next generation standards has become evident [15]. If in the past the scatterers and objects present in the environment were considered as obstructions and blockage structures for the EM signal propagation, it is now mandatory to introduce holistic wireless network design concepts in which the environment plays a fundamental role since it is becoming an essential degree-of-freedom (DoF) for the wireless planning and system design. According to such a vision, smart EM environments have been created by conceiving the use of artificial smart skins deployed/integrated on the walls of buildings to tailor the propagation of the EM waves in complex urban scenarios [16–19]. These skins consist of passive and/or active fixed/reconfigurable metasurfaces, specifically designed and fabricated, that can be suitable reconfigured by acting on simple electronic devices (e.g., radio-frequency switches, varactors). Thanks to their reconfiguration properties and the consequent need of developing ad-hoc intelligent reconfiguration techniques, the intelligent reflecting surfaces (IRSs) [16] are nowadays opening the doors to a completely new research arena (widely unexplored) for future mobile communications. Although, promising, IRS-based reconfigurable metastructures will not be massively deployed until the introduction of cost-effective solutions.

The building of the smart EM environment is envisaged in this work from a different perspective [20]. More specifically, the objects present in the environment are considered as they are, without the introduction of additional coating materials or artificial skins, and their scattering capabilities are opportunistically exploited to obtain the desired EM field distribution in a target region of interest. Towards this end, the DoFs considered in the synthesis are the control points (i.e., amplifiers and phase shifters) of the primary source, namely the BTS antenna array, whose values are properly optimized with the goal of generating the desired complex EM field distribution in the target region thanks to the scattering obtained when properly illuminating the objects present in the scenario through the field generated from the primary source, thus inducing suitable currents on the scatterers. This strategy, although characterized by a reduced number of DoFs as compared to the use of IRSs, does not require additional costs or infrastructures to the current network systems albeit it needs advanced processing tools and optimization-based design techniques as well as the knowledge of the surrounding environment.

The paper is organized as follows. Section 2 describes the mathematical formulation of the problem and the proposed design methodology. Some representative numerical results are reported in Section 3 to assess the effectiveness of the proposed method and the idea of the opportunistic exploitation of the surrounding scatterers for building a smart EM environment. Finally, some concluding remarks are drawn (Section 4).

2. Mathematical Formulation

Let us consider the wireless scenario depicted in Figure 1 where a primary source $\underline{J}_{inc}(\underline{r})$, $\underline{r} \in \Psi$ ($\underline{r} = \{r, \theta, \phi\}$), that models a BTS antenna array composed of N radiators with reconfigurable amplitude and phase weights $\underline{w} = \{w_n;\ n = 1, \ldots, N\}$, is installed in front of K scatterers (e.g., buildings) with known permittivity, $\varepsilon(\underline{r})$, and conductivity, $\sigma(\underline{r})$, distributions. The electric field $\underline{E}_{inc}(\underline{r})$ generated in far-field from the BTS is given by

$$\underline{E}_{inc}(\theta, \phi) = \sum_{n=1}^{N} \underline{E}_n(\theta, \phi) w_n e^{jk\underline{r}_n \cdot \underline{\hat{a}}} \tag{1}$$

where $\underline{E}_n(\theta, \phi)$, $n = 1, \ldots, N$ is the embedded/active far-field pattern of the n-th antenna including the local mutual coupling interactions [13], $k = \frac{2\pi}{\lambda}$ is the wavenumber, λ being the working wavelength, $\underline{r}_n$ ($n = 1, \ldots, N$) is the position of the n-th antenna of the BTS array, and $\underline{\hat{a}} = \sin\theta\cos\phi\,\underline{\hat{x}} + \sin\theta\sin\phi\,\underline{\hat{y}} + \cos\theta\,\underline{\hat{z}}$ is the unit vector identifying an arbitrary direction (θ, ϕ).

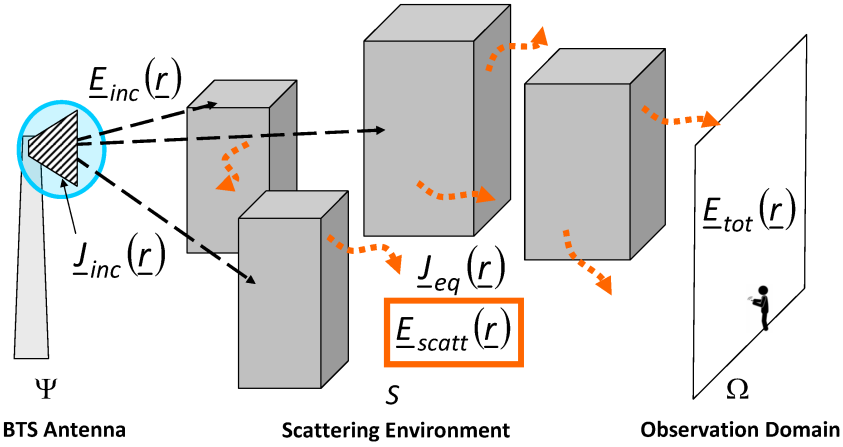

Figure 1. Smart EM environment.

By assuming the absence of EM coupling between the primary, $\underline{J}_{inc}(\underline{r})$, and the equivalent sources, $\underline{J}_{eq}(\underline{r})$, induced from the incident field $\underline{E}_{inc}(\underline{r})$ generated by the BTS on the scatterers lying in the environment S, the total electric field $\underline{E}_{tot}(\underline{r}) = \underline{E}_{inc}(\underline{r}) + \underline{E}_{scatt}(\underline{r})$ [21] is measured at M sampling positions $\underline{r}_m \in \Omega$, being Ω an external observation domain (Figure 1) where the end-user terminals are located. Moreover, $\underline{E}_{scatt}(\underline{r})$ is the electric field generated by $\underline{J}_{eq}(\underline{r})$ and mathematically expressed in the observation domain Ω as [21]

$$\underline{E}_{scatt}(\underline{r}_m) = j2\pi f \mu_0 \int_S \underline{\underline{G}}(\underline{r}_m | \underline{r}') \cdot \underline{J}_{eq}(\underline{r}') d\underline{r}' \tag{2}$$

where $\underline{J}_{eq}(\underline{r}) = \tau(\underline{r})\underline{E}_{tot}(\underline{r})$, $\underline{r} \in S$, and

$$\tau(\underline{r}) = [\varepsilon(\underline{r}) - 1] - j\frac{\sigma(\underline{r})}{2\pi f \epsilon_0} \tag{3}$$

is the so-called object function, $\underline{\underline{G}}(\underline{r}_m | \underline{r}')$ is the Green function, f is the operation frequency, $j = \sqrt{-1}$, and ϵ_0, μ_0 are the dielectric permittivity and the permeability constants of the free space, respectively.

In order to guarantee the desired coverage within Ω, the scattering environment is opportunistically exploited and the design problem is formulated as the synthesis of the set of complex weights $\underline{w}$ of the BTS antenna array such that a desired target field distribution $\underline{E}_{tar}(\underline{r}_m)$, $\underline{r}_m \in \Omega$, $m = 1, \ldots, M$ (M being the number of probing locations in Ω), is obtained. Towards this aim, due to the nonlinearity and ill-posedness of the arising

problem, the solution of the synthesis is cast as the optimization (i.e., the minimization) of the following cost function

$$\Phi(\underline{w}) = \sum_{p=\{x,y,z\}} \gamma_p \Phi_p(\underline{w}) \tag{4}$$

$\gamma_p \geq 0$, $p = \{x, y, z\}$ being real coefficients and

$$\Phi_p(\underline{w}) = \frac{\sum_{m=1}^{M} \left| E^p(\underline{r}_m|\underline{w}) - E^p_{tar}(\underline{r}_m) \right|^2}{\sum_{m=1}^{M} \left| E^p_{tar}(\underline{r}_m) \right|^2} \tag{5}$$

where $E^p(\underline{r}_m|\underline{w})$ and $E^p_{tar}(\underline{r}_m)$ are the p-th ($p = \{x, y, z\}$) component of the electric field obtained in Ω by controlling $\underline{J}_{inc}(\underline{r})$ and of the target electric field, respectively. The minimization of (4) is carried out by means the Particle Swarm Optimization (PSO), that is an effective global optimization algorithm [22] suitable for the minimization of multimodal and nondifferentiable cost function (5), in order to determine the optimal solution.

$$\underline{w}_{opt} = \arg\left\{ \min_{\underline{w}} [\Phi(\underline{w})] \right\} \tag{6}$$

3. Numerical Assessment

This section is aimed at numerically assessing the effectiveness and the potentialities of the proposed design framework. Towards this goal, an illustrative proof-of-concept is described by considering the benchmark scenario shown in Figure 2.

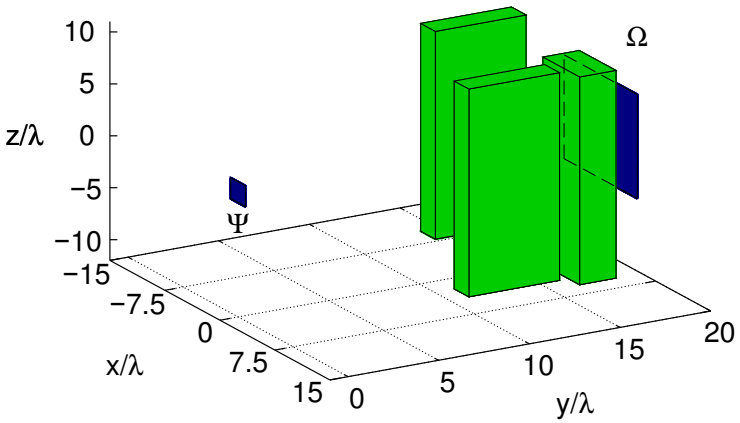

Figure 2. *Numerical Assessment* ($K = 3$, $N = 25$, $N' = 64$, $M = 441$)—Simulated benchmark scenario.

The *EM* environment $\mathcal{S}$ comprises $K = 3$ electrically-large scatterers (i.e., the maximum edge measures $L_{\max} = L_z = 20$ [λ], λ being the free-space wavelength at the working frequency) whose size and location is reported in Table 1, while their dielectric characteristics are set to concrete (i.e., relative permittivity $\varepsilon_r = 7.0$ and conductivity $\sigma = 0.015$ [S/m] [23]).

Table 1. *Numerical Assessment* ($K = 3$, $N = 25$, $N' = 64$)—Size and location of the scatterers within $\mathcal{S}$.

Scatterer k	**Size** $\left(L_x^{(k)}, L_y^{(k)}, L_z^{(k)}\right)$ [λ]	**Barycenter** $\left(x^{(k)}, y^{(k)}, z^{(k)}\right)$ [λ]
1	(5.0, 2.0, 20.0)	(7.0, 16.0, 0.0)
2	(2.0, 5.0, 20.0)	(7.0, 12.0, 0.0)
3	(5.0, 5.0, 20.0)	(−5.0, 15.0, 0.0)

As for the incident current distribution, $\underline{J}_{inc}(\underline{r})$, $\underline{r} \in \Psi$, it is that of a planar phased array of $N = (5 \times 5) = 25$ z-directed half-wavelength dipole antennas lying on the (x, z) plane and centered on the Cartesian axes origin (Figure 2) (Owing to the intrinsic linear polarization of the considered source and without any loss of generality, the scalar z-component of the electric field has been considered in the following by setting the weights in the cost function equal to $\gamma_x = \gamma_y = 0.0$ and $\gamma_z = 1.0$). The observation domain Ω is a square planar surface of size $L_\Omega = 10$ $[\lambda]$ located beyond the scattering environment $\mathcal{S}$ at a distance $d_{\Psi\Omega} = 20$ $[\lambda]$ from the source (Figure 2). The *EM* field within Ω has been sampled with uniform step along x and z directions with probing step $\Delta_x = \Delta_y = \frac{\lambda}{2}$, yielding a total number of measurement samples equal to $M = (21 \times 21) = 441$. Due to the large scale of the scenario at hand, a ray-tracing numerical solver based on the physical optics tool of Altair FEKO has been adopted to efficiently simulate the *EM* interactions, including the multipath, between the primary source and the scatterers [24]. Finally, the following parameters have been set to run the optimization: $P = 10$ (number of particles), $I = 10^4$ (maximum number of iterations), $\omega = 0.4$ (constant inertial weight), and $C_1 = C_2 = 2.0$ (acceleration coefficients) [22]. The goal of the problem at hand is to synthesize a suitable equivalent current distribution $\underline{J}_{eq}(\underline{r})$ within $\mathcal{S}$ such that the field in Ω matches a target distribution corresponding to the field that would be radiated in free-space by a significantly larger aperture comprising $N' = (8 \times 8) = 64$ dipoles ($\frac{N'}{N} = 256\%$), whose magnitude and phase are reported in Figure 3a,b, respectively.

Figure 4a shows the evolution of the cost function $\frac{\Phi_i}{\Phi_1}$, $i = 1, \ldots, I$, Φ_1 being the value of Φ at the initial iteration, in which uniform excitations (i.e., $w_n = 1.0$, $n = 1, \ldots, N$) have been exploited to set an "initial guess" for the successive solution space exploration. As it can be observed, the mismatch between the synthesized and the target distributions has been remarkably reduced during the optimization process as pointed out by the final value of the $\frac{\Phi_i}{\Phi_1}$ ratio (i.e., $\left.\frac{\Phi_i}{\Phi_1}\right|_{i=I} = 4.6 \times 10^{-2}$—Figure 4). Such an outcome is qualitatively and pictorially evident by looking at the corresponding field distributions in Figure 3, afforded when exciting the dipole antennas of the BTS array with the PSO-retrieved amplitude and phase weights shown in Figure 4b. More specifically, Figure 3c,d and Figure 3e,f show the distribution of the magnitude [Figure 3c,e] and phase [Figure 3d,f] of the electric field afforded by the planar array of $N = 25$ dipoles in Ω when feeding the antennas uniformly and with optimal set of weights synthesized by means of the PSO, respectively. Thanks to the optimally-excited equivalent current distribution within the scattering environment, the resulting final distribution in Ω [$E_{opt}(\underline{r})$—Figure 3e,f] is significantly closer to the target one [$E_{tar}(\underline{r})$—Figure 3a,b] than the uniformly-excited case [$E_{uni}(\underline{r})$—Figure 3c,d]. It is worth remarking that such a good matching has been yielded both in magnitude [$\left|E_{opt}(\underline{r})\right|$ vs. $|E_{tar}(\underline{r})|$—Figure 3e vs. Figure 3a] and phase [$\angle E_{opt}(\underline{r})$ vs. $\angle E_{tar}(\underline{r})$—Figure 3f vs. Figure 3b], as clearly proved by the comparison between the plot of the corresponding error map [i.e., $\Delta E_{opt}(\underline{r}) = E_{opt}(\underline{r}) - E_{tar}(\underline{r})$—Figure 5b] and that of the initial guess solution [i.e., $\Delta E_{uni}(\underline{r}) = E_{uni}(\underline{r}) - E_{tar}(\underline{r})$—Figure 5a] shown in Figure 5.

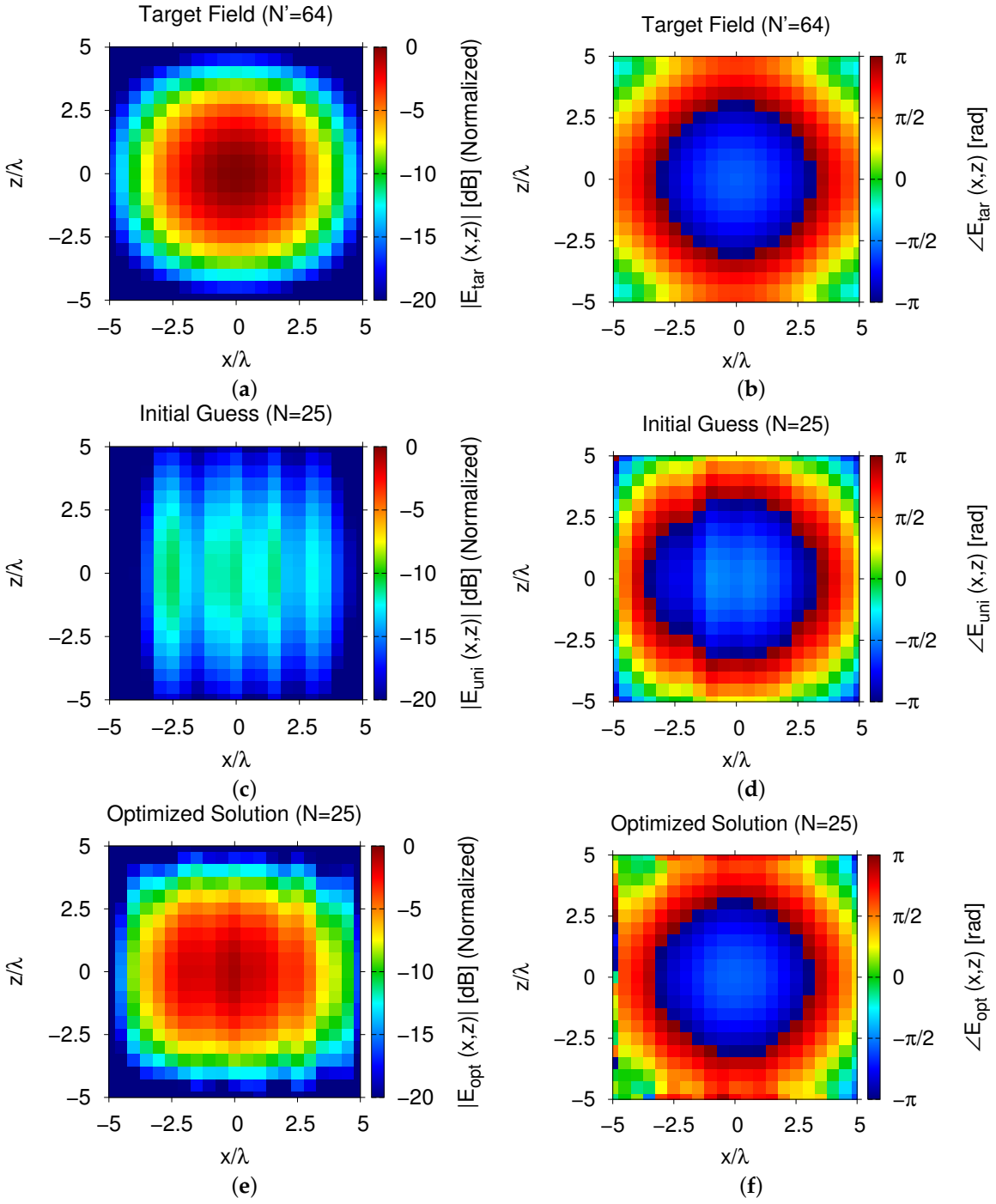

Figure 3. *Numerical Assessment* ($K = 3$, $N = 25$, $N' = 64$)—(**a**,**c**,**e**) Magnitude and (**b**,**d**,**f**) phase distribution of (**a**,**b**) the target field ($N' = 64$ dipoles in free-space) and the field radiated towards the complex scattering scenario $\mathcal{S}$ by the planar array of $N = 25$ dipoles when exciting the antennas with (**c**,**d**) uniform ("initial guess") and (**e**,**f**) the optimized excitation weights $\underline{w}_{opt}$.

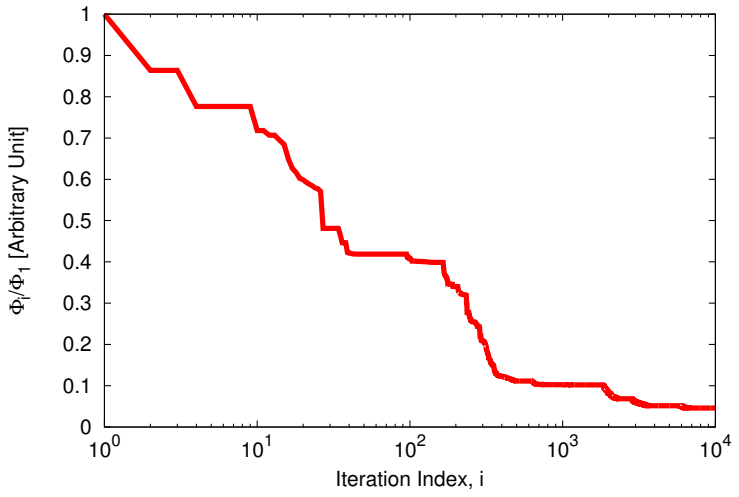

(**a**)

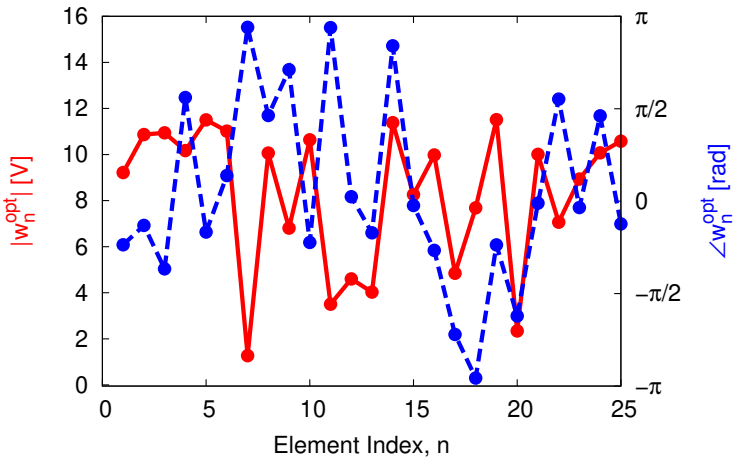

(**b**)

Figure 4. *Numerical Assessment* ($K = 3$, $N = 25$, $N' = 64$, $M = 441$)—Plot of (**a**) the evolution of the cost function during the iterations and (**b**) the amplitude $\left|w_n^{opt}\right|$, $n = 1, \ldots, N$ and phase $\angle w_n^{opt}$, $n = 1, \ldots, N$ values of the optimal excitations vector $\underline{w}_{opt}$ (6) obtained by means of the PSO.

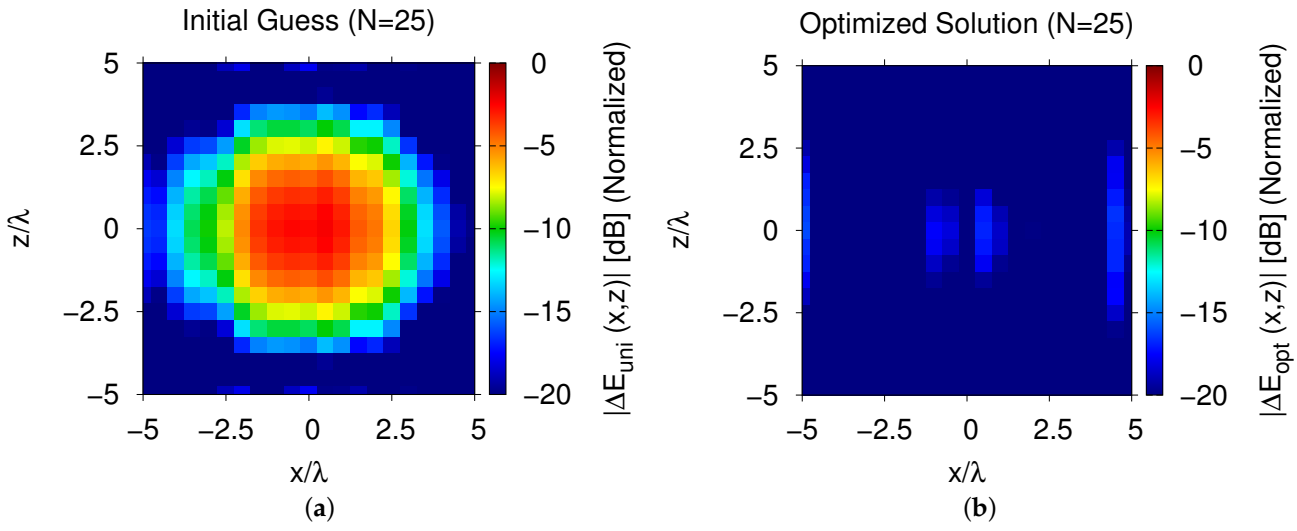

(**a**) (**b**)

Figure 5. *Numerical Assessment* ($K = 3$, $N = 25$, $N' = 64$, $M = 441$) - Error map for $\underline{r} \in \Omega$ between the target distribution and the field radiated by the array of $N = 25$ dipoles with (**a**) uniform $[\Delta E_{uni}(\underline{r}) = E_{uni}(\underline{r}) - E_{tar}(\underline{r})]$ and (**b**) optimized $[\Delta E_{opt}(\underline{r}) = E_{opt}(\underline{r}) - E_{tar}(\underline{r})]$ excitations.

4. Conclusions

Within the framework of the emerging "smart EM environments" paradigm for enabling next generation wireless communications systems, an optimization-based strategy for synthesizing a desired field distribution over a region of interest, where the end-user terminals are located, has been here introduced. Thanks to the complex scattering phenomena generated from the EM interactions of the primary source and the obstacles present in the scenario, supposed known and opportunistic exploited as passive metastructures, the configuration of the excitation weights controlling the field transmitted from a BTS has been properly synthesized by solving an optimization problem with the PSO to minimize a cost function quantifying the mismatch between the actual field generated in the region of interest and a target field distribution. The reported illustrative result has pointed out that it is possible to generate complex field distributions in the target region without recurring to the deployment of wider (i.e., more complex and expensive) free-space BTSs but just benefiting from the interactions between the EM field generated by the actual/standard BTS and the scattering objects.

Future research activities, beyond the scope of this paper, will be aimed at extending the proposed methodology to consider scenarios that are not deterministically known, for example by taking into account statistical propagation models, with the inclusion of moving scatterers. Moreover, future advances will be devoted to improving the efficiency of the method in terms of field computation, now representing one of the key computational issues in the optimization stage and to consider as target the power values or the EM field strength since telecommunications' operators usually want to obtain a power level at the receivers higher than a threshold rather than a complex EM field distribution.

Author Contributions: All authors contributed equally to this work. All authors have read and agreed to the published version of the manuscript.

Funding: This work has been partially supported by the Ministry of Education of China within the Chang-Jiang Visiting Professor chair and by the Italian Ministry of Education, University, and Research within the Program PRIN 2017 (CUP: E64I19002530001) for the Project CYBER-PHYSICAL ELECTROMAGNETIC VISION: Context-Aware Electromagnetic Sensing and Smart Reaction (EMvisioning) (Grant no. 2017HZJXSZ) and for the Project CLOAKING METASURFACES FOR A NEW GENERATION OF INTELLIGENT ANTENNA SYSTEMS (MANTLES) (Grant no. 2017BHFZKH).

Institutional Review Board Statement: Not applicable.

Informed Consent Statement: Not applicable.

Data Availability Statement: The data presented in this study are available on request from the corresponding author.

Conflicts of Interest: The authors declare no conflict of interest.

References

1. Liu, D.; Hong, W.; Rappaport, T.S.; Luxey, C.; Hong, W. What will 5G antennas and propagation be? *IEEE Trans. Antennas Propag.* **2017**, *65*, 6205–6212. [CrossRef]
2. Akyildiz, I.F.; Kak, A.; Nie, S. 6G and beyond: The future of wireless communications systems. *IEEE Access* **2020**, *8*, 133995–134030. [CrossRef]
3. Nawaz, S.J.; Sharma, S.K.; Wyne, S.; Patwary, M.N. Asaduzzaman Quantum machine learning for 6G communication networks: State-of-the-art and vision for the future. *IEEE Access* **2019**, *7*, 46317–46350. [CrossRef]
4. Viswanathan, H.; Mogensen, P.E. Communications in the 6G era. *IEEE Access* **2020**, *8*, 57063–57074. [CrossRef]
5. Yaacoub, E.; Alouini, M. A key 6G challenge and opportunity—Connecting the base of the pyramid: A survey on rural connectivity. *Proc. IEEE* **2020**, *108*, 533–582. [CrossRef]
6. Bariah, L.; Mohjazi, L.; Muhaidat, S.; Sofotasios, P.C.; Kurt, G.K.; Yanikomeroglu, H.; Dobre, O.A. A prospective look: Key enabling technologies, applications and open research topics in 6G networks. *IEEE Access* **2020**, *8*, 174792–174820. [CrossRef]
7. Ziegler, V.; Viswanathan, H.; Flinck, H.; Hoffmann, M.; Raisanen, V.; Hatonen, K. 6G architecture to connect the worlds. *IEEE Access* **2020**, *8*, 173508–173520. [CrossRef]

8. Chowdhury, M.Z.; Shahjalal, M.; Ahmed, S.; Jang, Y.M. 6G wireless communication systems: Applications, requirements, technologies, challenges, and research directions. *IEEE Open J. Commun. Soc.* **2020**, *1*, 957–975. [CrossRef]
9. Grande, M.; Bianco, G.V.; Laneve, D.; Capezzuto, P.; Petruzzelli, V.; Scalora, M.; Prudenzano, F.; Bruno, G.; D'Orazio, A. Optically transparent wideband CVD graphene-based microwave antennas. *Appl. Phys. Lett.* **2018**, *112*, 251103. [CrossRef]
10. Rocca, P.; Oliveri, G.; Mailloux, R.J.; Massa, A. Unconventional phased array architectures and design methodologies—A review. *Proc. IEEE* **2016**, *104*, 544–560. [CrossRef]
11. Herd, J.S.; Conwey, M.D. The evolution to modern phased array architectures. *Proc. IEEE* **2016**, *104*, 519–529. [CrossRef]
12. Oliveri, G.; Gottardi, G.; Robol, F.; Polo, A.; Poli, L.; Salucci, M.; Chuan, M.; Massagrande, C.; Vinetti, P.; Mattivi, M.; et al. Co-design of unconventional array architectures and antenna elements for 5G base stations. *IEEE Trans. Antennas Propag.* **2017**, *65*, 6752–6767.
13. Mailloux, R.J. *Phased Array Antenna Handbook*, 3rd ed.; Artech House: Norwood, MA, USA, 2018. [CrossRef]
14. Oliveri, G.; Gottardi, G.; Massa, A. A new meta-paradigm for the synthesis of antenna arrays for future wireless communications. *IEEE Trans. Antennas Propag.* **2019**, *67*, 3774–3788. [CrossRef]
15. Xu, C.; Yang, L.; Zhang, P. Practical backscatter communication systems for battery-free internet of things: A tutorial and survey of recent research. *IEEE Signal Proc. Mag.* **2018**, *35*, 16–27. [CrossRef]
16. Basar, E.; Di Renzo, M.; De Rosny, J.; Debbah, M.; Alouini, M.-S.; Zhang, R. Wireless communications through reconfigurable intelligent surfaces. *IEEE Access* **2019**, *7*, 116753–116773. [CrossRef]
17. Di Renzo, M.; Song, J. Reflection probability in wireless networks with metasurface-coated environmental objects: An approach based on random spatial processes. *EURASIP J. Wirel. Commun. Netw.* **2019**, *99*, 1–15. [CrossRef]
18. Di Renzo, M.; Debbah, M.; Phan-Huy, D.-T.; Zappone, A.; Alouini, M.-S.; Yuen, C.; Sciancalepore, V.; Alexandropoulos, G.C.; Hoydis, J.; Gacanin, H.; et al. Smart radio environments empowered by reconfigurable AI meta-surfaces: An idea whose time has come. *EURASIP J. Wirel. Commun. Netw.* **2019**, *129*, 1–20. [CrossRef]
19. Pengnoo, M.; Barros, M.T.; Wuttisittikulkij, L.; Butler, B.; Davy, A.; Balasubramaniam, S. Digital twin for metasurface reflector management in 6G terahertz communications. *IEEE Access* **2020**, *8*, 114580–114596.
20. Salucci, M.; Li, B.; Benoni, A.; Rocca, P.; Massa, A. Smart EM environment as enabling technology for future wireless systems. In Proceedings of the 14th International Congress on Artificial Materials for Novel Wave Phenomena (Metamaterials' 2020), New York, NY, USA, 28 September–3 October 2020; pp. 48–50.
21. Bertero, M.; Boccacci, P. *Introduction to Inverse Problems in Imaging*; IOP Press: Bristol, UK, 1998. [CrossRef]
22. Rocca, P.; Benedetti, M.; Donelli, M.; Franceschini, D.; Massa, A. Evolutionary optimization as applied to inverse problems. *Inverse Probl.* **2009**, *25*, 1–41. [CrossRef]
23. Robert, A. Dielectric permittivity of concrete between 50 MHz and 1 GHz and GPR measurements for building materials evaluation. *J. Appl. Geophys.* **1998,** *40*, 89–94.
24. Altair Feko. Available online: https://www.altair.com/feko/ (accessed on 10 May 2021).